Journal of Cerebral Blood Flow & Metabolism (2011) 31, 1612–1622

www.jcbfm.com

Brain energization in response to deep brain stimulation of subthalamic nuclei in Parkinson's disease

Gaëtan Garraux[1,2], Mohamed A Bahri[1], Christian Lemaire[1], Christian Degueldre[1], Eric Salmon[1,2] and Bruno Kaschten[3]

[1]*Cyclotron Research Center, University of Liege, Liège, Belgium;* [2]*Department of Neurology, University Hospital Center, Liège, Belgium;* [3]*Department of Neurosurgery, University Hospital Center, Liège, Belgium*

Deep brain stimulation (DBS) of the subthalamic nucleus (STN) is an effective treatment in a subgroup of medically refractory patients with Parkinson's disease (PD). Here, we compared resting-state ^{18}F-fluorodeoxyglucose (FDG) positron emission tomography images in the stimulator off (DBS_OFF) and on (DBS_ON) conditions in eight PD patients in an unmedicated state, on average 2 years after bilateral electrode implantation. Global standardized uptake value (SUV) significantly increased by ~11% in response to STN-DBS. To avoid any bias in the voxel-based analysis comparing DBS_ON and DBS_OFF conditions, individual scan intensity was scaled to a region where FDG-SUV did not differ significantly between conditions. The resulting FDG-SUV ratio (FDG-SUVR) was found to increase in many regions in response to STN-DBS including the target area of surgery, caudate nuclei, primary sensorimotor, and associative cortices. Contrary to previous studies, we could not find any regional decrease in FDG-SUVR. These findings were indirectly supported by comparing the extent of areas with depressed FDG-SUVR in DBS_OFF and DBS_ON relatively to 10 normal controls. Altogether, these novel results support the prediction that the effect of STN-DBS on brain activity in PD is unidirectional and consists in an increase in many subcortical and cortical regions.
Journal of Cerebral Blood Flow & Metabolism (2011) **31,** 1612–1622; doi:10.1038/jcbfm.2011.41; published online 6 April 2011

Keywords: FDG uptake; neurosurgery; Parkinson's disease; positron emission tomography; SUV

Introduction

High-frequency electrical stimulation of the subthalamic nucleus (STN) area is an established treatment option in a carefully selected subgroup of nondemented patients with advanced Parkinson's disease (PD) who suffer from significant dyskinesias and motor fluctuations despite optimal medical management. Over the last decade, there has been cumulative evidence supporting a sustained beneficial effect of deep brain stimulation (DBS) of the STN area on various disabling symptoms in PD (Krack *et al*, 2003; Fasano *et al*, 2010).

Yet, the underlying neural mechanisms remain unclear. Much research has focused on how STN-DBS affects brain activity. The most commonly employed paradigm involves the comparison of brain activity measured postoperatively in the stimulator off (DBS_OFF) and on (DBS_ON) conditions using electrophysiology or brain imaging in the resting-state or as patients are engaged in perceptual, cognitive, or motor tasks (Ballanger *et al*, 2009).

Here, we used ^{18}F-fluorodeoxyglucose (FDG) positron emission tomography (PET) to compare resting-state FDG uptake between DBS_OFF and DBS_ON conditions in eight patients with PD in an unmedicated state, on average 2 years after bilateral electrode implantation in the STN area. In the absence of arterial blood sampling, we were not able to obtain absolute values of the cerebral metabolic rate of glucose. FDG-PET data quantification was approximated by using standardized uptake values (SUVs) obtained by a normalization of FDG uptake to the total amount of tracer injected and the participant's body weight (Thie, 2004).

The STN-DBS-induced changes in FDG uptake or resting-state regional cerebral blood flow have already been extensively studied using PET and single photon emission tomography (SPECT) but

Correspondence: Dr G Garraux, MoVeRe Group, Department of Neurology, Cyclotron Research Centre, University of Liège, Sart Tilman B30, 4000 Liège, Belgium.
E-mail: ggarraux@ulg.ac.be
This work was supported by FRS-FNRS and a grant from the Rahier Foundation, University of Liège, Belgium.
Received 22 November 2010; revised 3 March 2011; accepted 4 March 2011; published online 6 April 2011

results have often been inconsistent across studies with respect to the precise distribution and direction (i.e., increases and decreases) of these changes. The most frequently reported finding is a relative decrease in primary sensorimotor cortex (S1M1) activity (Limousin *et al*, 1997; Payoux *et al*, 2004; Trost *et al*, 2006; Asanuma *et al*, 2006) in DBS_ON, the magnitude of which was found to be proportional to the frequency of stimulation (Haslinger *et al*, 2005). However, these results are difficult to reconcile with current models of basal ganglia cortical circuits, which predict an overall increase in motor cortical activity in response to STN-DBS (DeLong, 1990). By combining quantitative FDG-PET data with anatomical magnetic resonance imaging (MRI), Hilker *et al* (2008) showed that STN-DBS increased the normalized regional resting cerebral metabolic rate of glucose in the target area of surgery. In other areas, both increases and decreases have been reported including in the thalamus (Ceballos-Baumann *et al*, 1999; Hilker *et al*, 2004; Asanuma *et al*, 2006; Karimi *et al*, 2008; Arai *et al*, 2008), lentiform nucleus (Hilker *et al*, 2004; Arai *et al*, 2008), cerebellum (Hilker *et al*, 2004; Vafaee *et al*, 2004; Asanuma *et al*, 2006), lateral/medial premotor areas (Sestini *et al*, 2002; Trost *et al*, 2006), as well in associative fronto-temporo-parietal cortices (Ceballos-Baumann *et al*, 1999; Sestini *et al*, 2002; Hilker *et al*, 2004). These inconsistent observations may result from many factors, including the PD patients' demographic and clinical characteristics, time elapsed between DBS surgery and imaging, electrode position within the STN area, stimulation settings, and methodological aspects of PET/SPECT data acquisition and analysis.

With respect to the imaging methods, we hypothesized that the interpretation of DBS-induced changes (i.e., DBS_ON versus DBS_OFF) on regional FDG-SUV would greatly benefit from the choice of an appropriate reference region to normalize images intensity before their analysis. Intensity normalization of regional tracer uptake to the uptake in a reference area is commonly employed in PET and SPECT data analyses to account for intersubject and intrasubject variability associated with various sources of physiological and nonphysiological noise (Friston *et al*, 1990). In virtually all previous studies comparing brain activity in DBS_ON and DBS_OFF conditions, individual PET or SPECT images were scaled to their global mean (GM), whether quantitative data were available (Hilker *et al*, 2004, 2008; Asanuma *et al*, 2006) or not (Arai *et al*, 2008; Wang *et al*, 2010). Yet, it has been shown that the use of the GM as a scaling factor (i.e., in the denominator) may artificially increase regional FDG uptake or blood flow in images where the global activity is more severely affected (Borghammer *et al*, 2009) as in nondemented patients with advanced PD studied in the off condition (Eidelberg *et al*, 1994). An 8% to 10% difference in the GM between groups is sufficient to introduce such a bias in the analysis of GM normalized images. Here, we provide evidence, suggesting that STN-DBS significantly increases global FDG-SUV by $\sim$11%, prompting us to scale PET images to a reference region where the level of FDG-SUV did not significantly differ between the two stimulation conditions. This region was identified using the method proposed by Yakushev *et al* (2009). In the remaining sections, we will refer to these as FDG-SUV ratio (FDG-SUVR) images. Contrary to previous studies, the voxel-by-voxel paired *t*-test analysis of these images could not identify any region where FDG-SUVR decreased in DBS_ON as compared with DBS_OFF including in the S1M1 area.

The present work also differs methodologically from most earlier studies by the inclusion of FDG-PET scans from 10 healthy elderly controls (CONT). The comparison between FDG uptake in controls and FDG uptake changes in response to STN-DBS has only been investigated by a small number of studies (Hilker *et al*, 2004). Based on the results of the aforementioned paired *t*-test analysis and the consistent observations that individuals with advanced PD are characterized by widespread decreases in cortical and subcortical FDG uptake (Eidelberg *et al*, 1994; Berding *et al*, 2001), we predicted that STN-DBS decreases the extent of the relative hypometabolism in PD as compared with controls.

Finally, we investigated if the results of these voxel-based analyses were supported by those of volumes of interest (VOIs) centered on regions that are likely to have an important role in mediating the therapeutic effects of STN-DBS: the STN and S1M1 areas. These VOIs were defined *a priori* on the basis of anatomical landmarks (i.e., electrode artifact in the vicinity of the target area of surgery and hand knob in the central sulcus, respectively) visualized on the group mean spatially normalized postoperative MRI obtained in six PD patients (Figure 1).

Materials and methods

We enrolled eight nonconsecutive patients with advanced PD who successfully underwent bilateral STN-DBS (Table 1) and 10 normal volunteers matched for age and gender (4F; mean age $\pm$ s.d., 59.7 $\pm$ 8.4 years). None of the control subjects had any history of neurologic dysfunction and none of them had complaints or evidence of movement disorder or cognitive deterioration at medical interview. However, no detailed evaluation of the cognitive status was available in any control participant at the time of PET assessment. Parkinson's disease patients were selected from a small cohort of operated patients who attended our clinic between December 2003 and October 2004 and agreed to participate in the study. The main inclusion criterion was a clinical improvement larger than 30% in the Unified Parkinson's Disease Rating Scale (UPDRS) III between DBS_ON and DBS_OFF after cessation of antiparkinsonian medications for 12 hours. We excluded patients with any evidence of dementia (Emre *et al*, 2007)

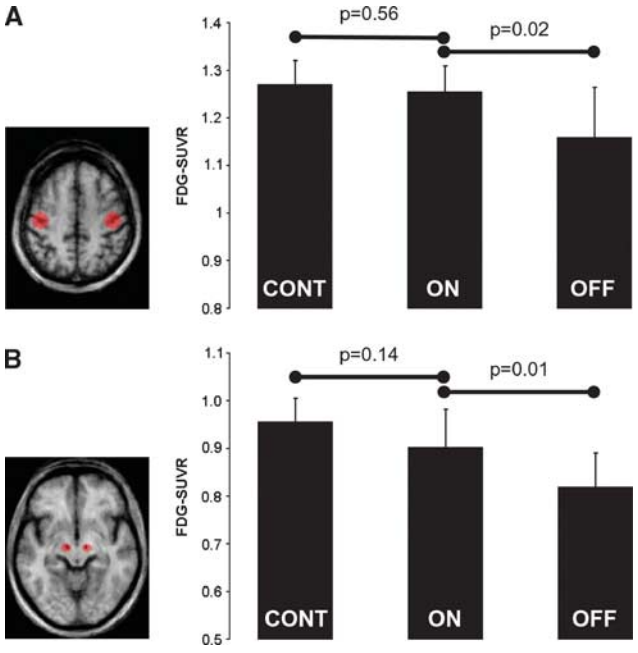

Figure 1 Volume of interest (VOI) analysis of FDG-SUVR in S1M1 and STN areas. (Left) *A priori* defined VOIs on bilateral S1M1 (**A**) and STN (**B**) areas. The VOIs are overlaid on axial slices through the mean postoperative anatomical magnetic resonance imaging (MRI) in standard stereotaxic space from six patients. (Right) The plots show the mean FDG-SUVR in bilateral S1M1 (**A**) and STN (**B**) areas from the 10 healthy elderly subjects ('CONT') and eight Parkinson's disease (PD) patients studied in DBS_ON ('ON') and DBS_OFF ('OFF') conditions. Vertical bars represent the s.d. In the STN area, the results are consistent with that previously reported by Hilker *et al* (2008), namely an activation of the target area of surgery toward normal activity. We observed a similar activity profile in S1M1, which goes in the opposite direction to what has been reported so far in previous PET studies. The comparison of the magnitude difference in FDG-SUVR between patients and controls requires caution because FDG-SUVR is likely to be overestimated in the patients relatively to controls (see text).

Table 1 Patient's demographic and clinical characteristics

Patient #	*Gender*	*Age (years) at*			*UPDRS III DBS_OFF*	*UPDRS III DBS_ON*
		Dx	*Surgery*	*PET*		
1	M	40	49	51	64	36
2	M	32	48	52	79	16
3	F	62	70	72	49	21
4	M	54	64	65	55	32
5	M	60	74	76	47	27
6	F	47	64	66	39	27
7	M	53	64	66	77	32
8	M	46	55	56	41	24

Dx, diagnosis; F, female; M, male; PET, positron emission tomography; UPDRS, Unified Parkinson's Disease Rating Scale.
UPDRS III scores were all obtained after cessation of antiparkinsonian medications for 12 hours.

at the time of PET assessment. None of the participants had diabetes at inclusion. Informed verbal and written consents for this research protocol, which was approved by the local Ethic Committee, were obtained from all subjects before the study.

Patient screening and surgery were performed at the Liège University Hospital Centre, University Campus of Sart Tilman, Belgium. Parkinson's disease was diagnosed according to the UK Parkinson's Disease Society Brain Bank criteria (Hughes *et al*, 1992). Disease severity was measured with the UPDRS before surgery in a drug-on state and 12 hours after cessation of antiparkinsonian medications ('practically defined off state'). Patients also had a neuropsychological and neuropsychiatric evaluation before surgery to rule out dementia and severe depression. Any significant structural brain abnormality on the preoperative MRI scan was considered as an exclusion criterion.

Quadripolar electrodes (Medtronic model 3389) were implanted bilaterally into the STN in a single surgical procedure under local anesthesia using a target location technique combining presurgical steretotactic planning and macroelectrode stimulation. Correct electrode positioning was further documented on postoperative MRI and excellent clinical responses as assessed by the changes in UPDRS scores after DBS. The electrodes were connected to the impulse generator (one patient with two Itrel III and seven patients with Kinetra models, Medtronic Inc., Minneapolis, MN, USA) implanted subcutaneously in the pectoral region 1 week after electrode placement. During the follow-up period, medications and DBS parameters were optimized individually as a function of the patient's motor status. Global cognition was also assessed at follow-up visits after surgery using the minimental state exam (MMSE; maximum score = 30) (Folstein *et al*, 1975).

At the time of PET, which was performed on average 2 years after surgery (range 1 to 4 years), the clinical benefit of STN-DBS on motor symptoms was quantified in all PD patients by comparing UPDRS III scores in the OFF stimulation/OFF drug and ON stimulation/OFF drug conditions (Table 1). Stimulation characteristics are summarized in Supplementary Table 1.

Imaging Data Acquisition

Scintigraphic images of resting-state cerebral FDG uptake were all obtained at the Cyclotron Research Centre, University Campus of Sart Tilman, Belgium, with eyes closed on a SIEMENS CTI 951 R 16/31 tomograph (CTI, Knoxville, TN, USA) in two-dimensional mode, after fasting for at least 12 hours (Garraux *et al*, 1999). In the patient group, PD medications were withdrawn for at least 12 hours before PET scanning (practical drug-off state). Patients had two PET scans on two separate days: in DBS on (DBS_ON) and DBS off (DBS_OFF) conditions. Positron emission tomography scans were performed first in DBS_OFF or DBS_ON in six and two patients, respectively. This difference did not reach the statistical level of significance (Fisher exact, $P = 0.06$). The mean time interval between PET scans was 20 days for seven out of eight

patients. For one patient, the two PET scans were performed 146 days apart. There was no change in antiparkinsonian drug regimen or global health status between the two PET imaging sessions. The patients' clinical state was monitored by one of the investigators (BK) during PET. No patient had severe tremor or off-period dystonia that might have influenced cerebral FDG uptake.

Imaging Data Processing

After gross manual image reorientation and approximate definition of the image center point, the PET scans were spatially processed using the Statistical Parametric Mapping (SPM8) (http://www.fil.ion.ucl.ac.uk/spm/software/spm8/, Wellcome Trust Centre for Neuroimaging, London, UK) implemented in Matlab 7.4.0 (MathWorks, Natick, MA, USA).

All PET images were spatially normalized onto a study-specific FDG-PET template created on the basis of high-resolution T1-weighted MR images obtained in 'in house' controls and in six PD patients for whom the postoperative MR was available in an appropriate image format. Magnetic resonance imaging acquisition parameters were as follows: TR = 25 milliseconds, TE = 10 milliseconds voxel size = $0.89 \times 0.89 \times 1.2\,mm^3$; flip angle = 40°; matrix size was $256 \times 256 \times 128$ except in two patients in whom matrix size was $192 \times 256 \times 96$). Individual PET images were coregistered onto the corresponding individual MRI. The MRIs were segmented into different tissue classes and spatially normalized in SPM8 using DARTEL (Ashburner, 2007). Individual normalization parameters were then applied to the individually coregistered PET images, which were subsequently averaged and smoothed using an 8 mm FWHM kernel to create a study-specific FDG-PET template. All 26 PET images (10 in controls and 8 paired scans in PD) in native space were then spatially normalized onto this customized PET template, resliced into $3 \times 3 \times 3\,mm^3$ voxels and finally smoothed using a 12-mm FWHM kernel.

Imaging Data Analysis

Global FDG-SUV: We investigated whether or not STN-DBS affected global FDG-SUV by comparing images in DBS_ON and DBS_OFF conditions. A large VOI covering cerebral gray matter was defined by the binary mask image (56,778 voxels) generated by SPM in the paired *t*-test analysis comparing DBS_ON and DBS_OFF conditions (see below). The mean FDG-SUV in this large VOI was extracted on a scan-by-scan basis from spatially normalized and smoothed images using Marsbar v0.42 (Mathew Brett *et al*; freely available at http://sourceforge.net/projects/marsbar/files/).

The magnitude of the difference between DBS_ON and DBS_OFF conditions was computed as ((DBS_ON–DBS_OFF)/DBS_OFF × 100). Differences between CONT and PD were computed as ((PD–CONT)/CONT × 100). DBS_ON and DBS_OFF were compared statistically using the Wilcoxon signed-rank test, while differences between PD and CONT groups were assessed using the Mann–Whitney *U*-test. Statistical analyses were performed using Statistica (Statsoft, Maisons-Alfort, France; http://www.statsoft.fr/).

Statistical parametric mapping analyses of FDG-SUVR images: Voxel-based image analyses were conducted using SPM8 in the framework of the General Linear Model. Because DBS_ON and DBS_OFF conditions significantly differed in terms of global FDG-SUV (see below), we did not use the GM as a scaling factor before image analysis comparing DBS_OFF and DBS_ON conditions (Borghammer *et al*, 2009). Here, we identified regions where the FDG-SUV was mostly preserved in DBS_OFF as compared with DBS_ON using the cluster reference approach proposed by Yakushev *et al* (2009). We applied the same procedure for the comparison between DBS_OFF and controls (CONT). The reference cluster common to both analyses encompassed the left medial temporal area. Mean individual FDG-SUV in this cluster was extracted on a scan-by-scan basis in both PD and CONT groups using Marsbar v0.42. The group mean FDG-SUV in the cluster reference region did not differ significantly between DBS_ON and DBS_OFF conditions (difference = 3.1%; $P = 0.32$) but was significantly lower in DBS_ON (mean −28.6%; range −9% to −40.6%; $P = 0.003$) and DBS_OFF (mean −30.6%; range −9% to −47.6%; $P = 0.003$) as compared with CONT. Each scan was scaled by the corresponding metabolic value in this cluster using the proportional scaling procedure as implemented in SPM8.

Next, we conducted three SPM analyses on these FDG-SUVR images. The main analysis of the present study looked for regional differences in FDG-SUVR between DBS_ON and DBS_OFF conditions. This was modeled statistically using a voxel-by-voxel paired *t*-test in SPM8. Results were characterized in terms of the probability that the variation in magnitude value in a given voxel could occur by chance under the null hypothesis. Significance level was set at $P < 0.001$, uncorrected, for the peak with an extent threshold of 10 contiguous voxels.

Next, we tentatively performed two additional SPM analyses involving FDG-SUVR images from CONT to test the hypothesis that STN-DBS decreases the extent of the overall hypometabolism in PD as compared with controls. The spatial extent of the regional hypometabolism in PD was estimated by a comparison of the voxel count of hypometabolic clusters in 'CONT minus DBS_OFF' and 'CONT minus DBS_ON' analyses, both thresholded at $P < 0.001$, uncorrected. The search volume of these two SPM analyses was defined by the binary mask image (56,778 voxels) generated by SPM8 in the aforementioned paired *t*-test analysis. As discussed later, we acknowledge that the results of those analyses comparing FDG-SUVR images from PD and CONT are biased by a significant difference in FDG-SUV in the reference region between PD and CONT (Borghammer *et al*, 2009).

Volume of interest analyses of FDG-SUVR images: Spherical VOIs were created on *a priori* defined regions, namely the target area of surgery (STN areas) and S1M1. The left and right STN area and S1M1 spherical VOIs were created using Marsbar v0.42 on the basis of landmarks visualized on the group mean spatially normalized

postoperative MRI obtained in six PD patients. The S1M1 VOIs (10 mm radius) were centered on the presumed position of the hand representation area in the central sulcus. The STN VOIs (5 mm radius) were centered on the electrode artifact in the vicinity of the target area of surgery (Figure 1). We extracted the mean individual FDG-SUV in bilateral STN and S1M1 VOIs from spatially normalized and smoothed PET images. These VOI FDG-SUV were converted to FDG-SUVR by using a normalization to the FDG-SUV in the reference region (see above). Data were compared using the same procedure as that used for global FDG-SUV (see above).

Results

Clinical Data Analysis

The difference in UPDRS III (items 18 to 31 of the UPDRS) score between DBS_ON and DBS_OFF conditions at the time of PET imaging (Table 1) was significant ($P=0.012$). The group mean MMSE score at the time of PET and on average 81 months after DBS surgery (range 4 to 10 years) was 28.6 and 26.4, respectively.

Global FDG-SUV

Global FDG-SUV was on average 10.7% higher in the DBS_ON condition than in the DBS_OFF condition and this difference was significant ($P=0.02$). In comparison with CONT, global FDG-SUV was on average 31.8% lower in DBS_ON (range −12.6% to −44%; $P=0.002$) and 38.5% lower in DBS_OFF (range −20.5% to −50.9%; $P=0.001$). The differences with CONT are in the same order of magnitude as the ∼23% decrease in the global cerebral metabolic rate of glucose previously reported using quantitative FDG-PET in patients with advanced PD (Eidelberg *et al*, 1994).

Statistical Parametric Mapping Analyses of FDG-SUVR Images

The results of the paired *t*-test analysis comparing DBS_ON and DBS_OFF are presented in Figure 2 and Table 2. We were not able to find any region where STN-DBS decreased FDG-SUVR even at a liberal statistical threshold of $P<0.05$, uncorrected.

When compared with CONT, patients in the DBS_OFF condition were characterized by a decrease in FDG-SUVR in 27% of the search volume (Supplementary Figure 1). The total number of hypometabolic voxels in DBS_OFF as compared with CONT was 15,549 at a threshold of $P<0.001$, uncorrected. At the cortical level, hypometabolism was chiefly distributed in the lateral and medial parts of posterior associative cortices, the dorsolateral prefrontal cortex, both in its dorsal and ventral aspects, the medial prefrontal, anterior cingulate areas and the subgenual frontal cortex. Hypometabolism in subcortical structures was observed in the hypothalamus, cerebellum, pons, midbrain, infrathalamic areas including the target area of STN-DBS and in caudate nucleus and thalamus, bilaterally.

In DBS_ON, we found a restoration of control activity in 90% of these hypometabolic voxels (Supplementary Figure 2). A relative hypometabolism persisted during STN stimulation in a limited number of regions including the right posterior thalamic area, precuneus, bilateral posterior associative cortices, and bilateral prefrontal regions, mainly on the right. The total number of hypometabolic voxels in DBS_ON (in comparison with CONT) at $P<0.001$, uncorrected was 4,886.

This hypometabolic pattern was still present after excluding scans from three patients who developed prodromal dementia or dementia (Figure 3; Supplementary Table 2) as assessed at follow-up visits on clinical examination and performance at the MMSE (Emre *et al*, 2007).

Volume of Interest Analyses of FDG-SUVR Images

Plots of FDG-SUVR from bilateral S1M1 and STN VOIs in CONT and PD patients are given in Figure 1. S1M1 was not found to be overactive in DBS_OFF as compared with controls or DBS_ON. FDG-SUVR in the S1M1 VOIs was relatively decreased in DBS_OFF and increased by 8.4% in DBS_ON. FDG-SUVR increased by 10.2% in the STN VOIs in response to STN-DBS.

Discussion

The results observed in this FDG-PET study performed in eight nondemented patients with advanced PD support the prediction that the effect of STN-DBS on brain activity is unidirectional and consists in an increase in many subcortical and cortical regions. Contrary to previous studies, we were not able to identify any region where STN-DBS decreased FDG-SUVR. This apparent discrepancy might be explained by an important methodological difference in the choice of the reference area used to scale FDG-SUV images before their analysis. Furthermore, the increase in FDG-SUVR in response to STN-DBS was indirectly supported by the results of analyses comparing PET data in DBS_OFF and DBS_ON with those obtained in 10 normal controls. Decreased FDG-SUVR persisted in posterior associative cortices in DBS_ON but this was not predictive of dementia at follow-up on average 81 months after surgery. These novel results contribute to a better understanding of the mechanisms underlying STN-DBS clinical benefits/limitations and provide new data on PD pathophysiology.

Before we specifically address these points, we acknowledge that the present work has several

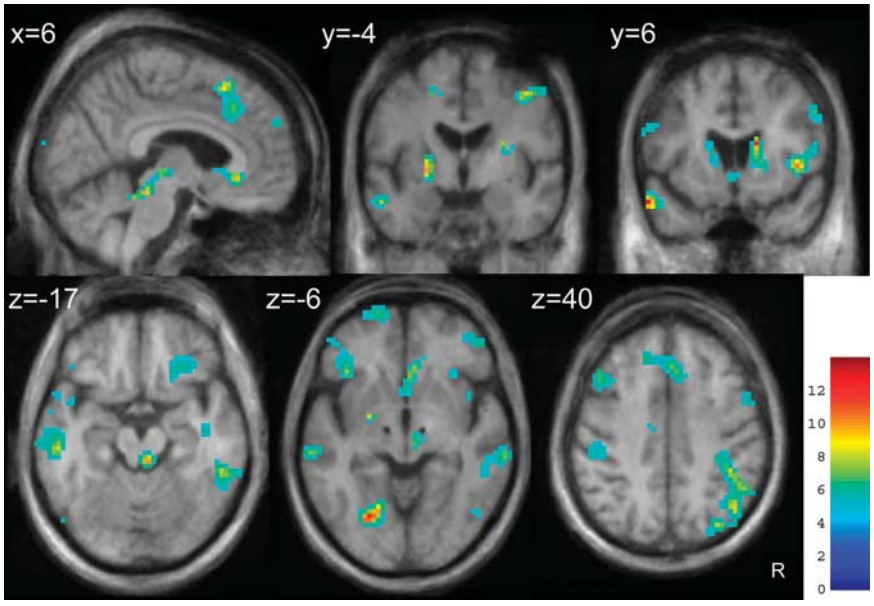

Figure 2 Brain areas where FDG-SUVR increased in DBS_ON as compared with DBS_OFF (SPM8 analysis). Statistical Parametric Mapping (SPM) results are superimposed on axial, coronal, and sagittal slices through the mean postoperative anatomical MRI in standard stereotaxic space from six patients, and thresholded at $P < 0.001$, uncorrected. Values in the upper left corner of each image indicate the distance (in millimeters) of the image from the axial plane through the anterior and posterior commissures (*z* values), from the coronal plane through the anterior commissure (*y* values), and from the parasagittal plane through the midline (*x* value). Note the black spots in upper brain stem ($z = -6$) corresponding to the mean electrode artifact on MR scans. Images are displayed in neurologic convention. The color scale represents the T statistics. R, right.

limitations. As in many previous neuroimaging studies (Limousin *et al*, 1997; Ceballos-Baumann *et al*, 1999; Hilker *et al*, 2004), the patient sample was low and the conclusions should be restricted to PD patients who benefit the most from STN-DBS as illustrated by the high level of improvement of UPDRS scores between the DBS_ON and DBS_OFF states at the time of scanning (Table 1). Another limitation is suboptimal PET sampling of the brain in the axial direction. Indeed, the vertex and bottom of cerebellum could not be imaged in all patients. As in several previous FDG-PET studies (Arai *et al*, 2008; Wang *et al*, 2010), quantitative PET data were not available and absolute values of cerebral metabolic rate of glucose could not be assessed. As an approximation, we measured FDG-SUV, which provides an assessment of cerebral FDG uptake normalized to the total amount of tracer injected and the patient's body weight (Thie, 2004). Blood glucose levels were not available at the time of PET despite this may influence FDG-SUV. We nevertheless assumed that, in a given patient, blood glucose levels were similar in DBS_ON and DBS_OFF conditions because PET scans were all performed using a standardized procedure after fasting for at least 12 hours and because none of the participants had diabetes at inclusion. Finally, we cannot exclude the possibility that the paired comparison of FDG-SUV in PD might be confounded by an order effect since PET data were acquired first in DBS_OFF or DBS_ON in six and two patients, respectively. However, this difference did not reach the level of statistical significance and the magnitude of the order effect, if any, is believed to be lower than that of STN-DBS (Maquet *et al*, 1990).

Global FDG-SUV significantly increased by ~11% in DBS_ON as compared with DBS_OFF. This difference is not trivial. It is in the same order of magnitude as the difference in the global cerebral metabolic rate of glucose between wakefulness and sleep (Nofzinger *et al*, 2002). To the best of our knowledge, quantification of STN-DBS-induced changes on global FDG uptake was not specifically reported in previous PET studies. Since FDG-SUV is a marker of glucose uptake, the main substrate for energy production in the brain, our results indicate that STN-DBS can be viewed as inducing a brain 'energization'. In the resting state, about 80% of basal glucose use is related to synaptic activity (Magistretti and Pellerin, 1999) and is proportional to synaptic density (Rocher *et al*, 2003). The exact anatomical relays and physiological mechanisms mediating this global increase in FDG uptake after a focal stimulation of the STN areas remain speculative. The remote and widespread cerebral metabolic effects of STN-DBS observed here are consistent with a restoration of normal functional coupling between distant brain areas demonstrated by electrophysiological recordings (Montgomery Jr and Gale, 2008), presumably requiring higher energy demands. Other mechanisms have been hypothesized including antidromic activation of cortical and subcortical

Table 2 Main brain regions where STN-DBS increased FDG-SUVR (SPM8 analysis)

	Right				*Left*			
	MNI coordinates[a]			Z *score*	*MNI coordinates*[a]			Z *score*
	x	y	z		x	y	z	
Lateral frontal cortex								
Orbitofrontal cortex	33	32	−20	3.68				
Fronto-polar cortex (BA10)	12	59	4	3.96	−21	65	1	4.33
Inferior frontal gyrus								
(BA47)	51	47	1	4.07	−39	38	−8	3.40
(BA10)	51	47	1	4.07	−48	47	1	3.71
Frontal operculum (BA44/45)	42	14	7	4.56				
Middle frontal gyrus								
(BA10)					−39	56	7	3.45
(BA9)					−45	23	40	3.59
(BA8)	39	20	55	3.41				
Superior frontal gyrus								
(BA10)	18	62	22	4.33	−18	59	22	3.87
(BA9)					−24	53	28	3.46
Precentral gyrus (BA6)	39	−7	46	3.91	−54	2	31	3.46
Insula (posterior)	42	−13	−14	3.65				
Lateral temporal cortex								
Left temporal pole (BA38)					−57	11	−23	4.55
Superior temporal gyrus (BA22)					−63	−28	1	3.88
Middle temporal gyrus (BA21)	63	−40	−14	4.16	−69	−22	−11	3.94
Inferior temporal gyrus (BA20)					−57	−27	−26	3.80
Fusiform gyrus (BA37)					−30	−31	−26	3.74
Lingual gyrus (BA18)					−24	−70	−5	4.52
Lateral parietal cortex								
Temporo-parietal junction	48	−49	40	3.78	−54	−46	31	3.59
Angular gyrus (BA39/40)	45	−64	40	4.12				
Inferior parietal lobule (BA40)	48	−49	40	3.78	−57	−43	40	4.05
Postcentral gyrus (BA1/2/3)	36	−31	43	3.58	−45	−25	34	3.45
Midline areas								
Subgenual frontal cortex (BA32/25)	6	29	−8	4.10				
Medial frontal gyrus								
(BA9)	0	47	31	3.84				
(BA10)	12	59	4	3.96				
(BA6—pre-SMA)	6	20	52	4.03				
Cingulate cortex								
Anterior (BA24/32)	12	26	19	3.42				
Middle (BA6/24; CCZ)					−12	−7	46	3.60
Cuneus (BA18)					−3	−94	16	4.51
Subcortical areas								
Caudate nucleus	18	20	7	3.97	−15	11	10	3.34
Left globus pallidus					−21	−4	−2	4.20
Thalamus	6	−22	−2	3.67	−18	−25	4	3.41
Right PPN area	6	−34	−17	4.21				
Left cerebellum					−12	−49	−23	3.48

ACC, anterior cingulate cortex; BA, Brodmann's area; CCZ, caudal cingulate zone; DBS, deep brain stimulation; PPN, pedunculopontine nucleus; pre-SMA, presupplementary motor area.

[a]Coordinates (in millimeters) of peak differences in MNI space (Montreal Neurological Institute; http://www.bic.mni.mcgill.ca) are given for information. Anatomical localization of SPM detected peak differences was assessed on the average spatially normalized MRI image from six patients with PD. Individual PET images were spatially normalized on a customized MRI-derived template that was specific for the data under investigation and thus that did not perfectly match the canonical template image in MNI space (see Materials and methods).

regions projecting to the STN (Montgomery Jr and Gale, 2008).

This significant increase in global FDG-SUV has important methodological implications for PET data analysis. A scaling procedure is commonly applied to PET/SPECT data images before their analysis to account for various sources of physiological and nonphysiological noise (Friston *et al*, 1990).

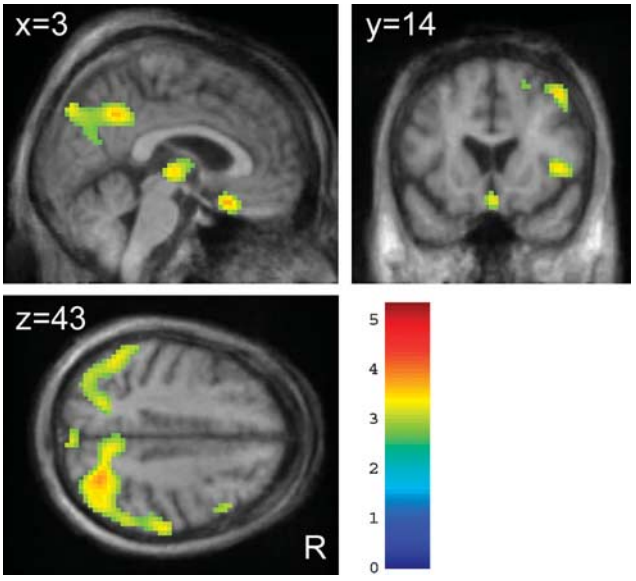

Figure 3 Areas of decreased FDG-SUVR in DBS_ON in the five patients without evidence of dementia at clinical follow-up. Results are presented at $P < 0.01$, uncorrected, for display purposes. Figure legend is the same as in Figure 2.

Different intensity normalization procedures have been proposed but none is systematically optimal in various neurodegenerative diseases. The most widely used procedure, including in virtually all previous FDG-PET studies examining the effects of STN-DBS in PD, is to scale individual image intensity to its GM (Asanuma *et al*, 2006; Hilker *et al*, 2008; Arai *et al*, 2008; Wang *et al*, 2010). However, the validity of this approach has been questioned when there is a large difference (i.e., >8% to 10%) in the GM between conditions as in the present study (see Introduction). Here, FDG-SUV images were scaled to a reference area where the difference in FDG-SUV was low (<5%) and not statistically significant between DBS_ON and DBS_OFF conditions. In other words, DBS_ON and DBS_OFF conditions were compared using FDG-SUVR images under the assumption that this analysis was unlikely to be biased by differences in FDG-SUV in the reference area used to scale image intensity before their analysis. As stated above, FDG-SUV only provides an approximation of the absolute FDG uptake and the results reported here should be replicated using quantitative FDG-PET data.

Nevertheless, this important methodological difference between the present study and previous ones in the choice of the reference area used to scale PET data before their analysis is likely to explain why we were not able to find a single gray-matter region where FDG-SUVR decreased in the voxel-based analysis comparing DBS_ON and DBS_OFF, even using a very liberal statistical threshold. For instance, we were not able to replicate the decrease in abnormal S1M1 activity previously reported in response to STN stimulation (Payoux *et al*, 2004; Trost *et al*, 2006; Asanuma *et al*, 2006; Geday *et al*, 2009). This is illustrated by the results the VOI analyses in bilateral S1M1 areas where the group mean FDG-SUVR significantly increased by 8.4% in response to STN-DBS (Figure 1A). Decreased FDG uptake has been previously reported in others areas in response to STN-DBS including in the lentifom nucleus (Arai *et al*, 2008; Wang *et al*, 2010), thalamus (Wang *et al*, 2010), lateral and medial parietal areas (Wang *et al*, 2010), but these observations are conflicting since other studies including ours reported STN-DBS-induced increases rather than decreases in these areas (Hilker *et al*, 2004; Asanuma *et al*, 2006).

In agreement with Hilker *et al* (2004), the present study provides evidence that many subcortical and cortical regions respond to STN-DBS by an increase in FDG uptake (Figure 2; Table 2). Consistent with a subsequent study of the same group (Hilker *et al*, 2008), STN-DBS increased activity in the target area of surgery. The group mean FDG-SUVR in the STN VOIs significantly increased by 10.2% in response to STN-DBS (Figure 1B). This novel finding adds to the evidence supporting the hypothesis that the beneficial effects of STN-DBS are mediated by an increased activity in the target area of surgery. As a corollary, these results confirm that hypometabolism in the STN area cannot be solely explained by a microlesional effect after electrode implantation (Hilker *et al*, 2008). The exact mechanisms underlying the STN area metabolic increase by DBS remain speculative but may involve a modulation of inputs to the STN (Hilker *et al*, 2008).

The positive FDG-PET response to STN-DBS extended to other basal ganglia regions: upper brain stem, thalamus, pallidum, and caudate nuclei. Because there is a large body of evidence supporting a role for the mesencephalic locomotor and pedunculopontine areas in the pathophysiology of freezing of gait in PD (Jenkinson *et al*, 2009), the finding in upper brain stem may be relevant in the understanding of mechanisms by which gait disturbances can be alleviated by STN-DBS. The present results also add to the existing evidence that STN-DBS increases FDG uptake in the globus pallidus (Hilker *et al*, 2008). Increased pallidal and PPN area FDG-SUVR could be mediated by excitatory projections from the STN.

Increased FDG-SUVR in caudate nuclei is a novel finding and may be secondary to the restoration of excitatory inputs from anatomically connected associative fronto-temporal associative network (Alexander and Crutcher, 1990) where FDG-SUVR also increased in response to STN-DBS (Figure 2; Table 2). Whereas the reported effects of STN-DBS on cognitive functions have been quite variable, ranging from worsening to improvement, results from Campbell *et al* (2008) and Kalbe *et al* (2009) both provided evidence, suggesting that this variability can be

predicted by STN-DBS-induced activity changes in the frontal cortex. At the time of PET, which was performed on average 2 years after DBS surgery, we had no indication that DBS altered cognitive functions in any of our patients, which is consistent with the observed increase in FDG-SUVR in the caudate nuclei and many anatomically related associative cortical regions. However, we cannot draw more precise conclusions because none of the patients was administered detailed cognitive testing at the time of PET scanning.

The increase in FDG-SUVR in response to STN-DBS in many subcortical and cortical regions was indirectly supported by the results of analyses comparing PET data in DBS_OFF and DBS_ON with those obtained in 10 normal controls. The widespread decreases in FDG-SUVR found here in patients in the DBS_OFF condition as compared with CONT (Supplementary Figure 1) supports results from previous PET studies in patients with advanced PD, which have demonstrated hypometabolism in upper brain stem, caudate nuclei (Berding *et al*, 2001), lateral temporo-parieto-occipital and precuneus/posterior cingulate regions (Berding *et al*, 2001; Hilker *et al*, 2004), the lateral premotor (Ma *et al*, 2007), dorsolateral prefrontal (Berding *et al*, 2001; Hilker *et al*, 2004), and ventro-medial and orbitofrontal cortices (Berding *et al*, 2001). Here, we observed that 90% of those hypometabolic voxels responded to STN-DBS by an increase in FDG-SUVR toward control levels. As previously reported by Hilker *et al* (2004), hypometabolism persisted in posterior cingulate, temporo-parieto-occipital cortices, and small lateral frontal clusters in the DBS_ON condition as compared with CONT (Supplementary Figure 2). These regions largely overlap with those found severely affected in demented PD patients (Lyoo *et al*, 2010). While no patients showed evidence of dementia at the time of PET scanning, three patients developed impaired global cognitive ability at MMSE (mean score = 21.6/30) and even dementia (Emre *et al*, 2007) at follow-up visits. The persistent hypometabolism in DBS_ON might therefore indicate prodromal dementia occurring independently from STN-DBS as a result of disease progression. To test that hypothesis, we repeated this analysis 'CONT minus DBS_ON' after exclusion of the three aforementioned patients. None of the five remaining individuals showed any evidence of dementia on clinical examination and all had normal MMSE score (mean = 29.2/30) at follow-up on average 81 months after surgery. Still, FDG-SUVR in medial and lateral parietal associative regions was significantly lower in these five patients than in CONT (Figure 3; Supplementary Table 2). Thus, in our small cohort, the pattern of decreased FDG-SUVR in DBS_ON relatively to CONT was not predictive of dementia within the time frame of follow-up. Clearly, the reason for (and consequence of) this persistent hypometabolic network in nondemented PD patients requires further investigation.

While we believe that the results of these analyses comparing PD and CONT are informative, we acknowledge some limitations. First, FDG-SUV in the reference area used to scale FDG-SUV images before their analysis was on average ~28% and ~30% lower in DBS_ON and DBS_OFF than in CONT, respectively. These differences are in the same order of magnitude as the decrease in the cerebral metabolic rate of glucose previously reported in a similar area using quantitative FDG-PET in patients with advanced PD (Eidelberg *et al*, 1994). This may lead to a systematic underestimation of the true hypometabolism when comparing FDG-SUVR images from PD and CONT (see above). Therefore, the results of the comparison between CONT and PD should be regarded as the areas where FDG-SUVR is the most affected in PD rather than the areas where FDG-SUVR is exclusively impaired. Second, no attempt was made to correct PET data for partial volume effects that may occur as a result of larger regional brain atrophy in PD patients as compared with CONT. However, these issues might not significantly affect the comparison of the *difference* between 'CONT minus DBS_ON' and 'CONT minus DBS_OFF' analyses because this potential bias is assumed to be similar in both analyses. Third, detailed cognitive evaluation was not available in CONT and we cannot exclude the possibility that some of these elderly individuals had very mild cognitive impairment (without cognitive complaint) at the time of PET scanning. However, this would have decreased the overall probability to find a significant difference between DBS_ON and CONT. Altogether we believe that these issues should not affect results interpretation of the comparisons between CONT and PD.

In conclusion, the present study provides evidence suggesting that STN-DBS significantly increases global cerebral FDG-SUV on average by ~11%. This result prompted us to scale FDG-SUV images to a reference region where the level of FDG-SUV did not significantly differ between DBS_ON and DBS_OFF conditions in subsequent voxel-based analyses. Contrary to previous studies, we could not find any region (i.e., S1M1) where STN-DBS decreased FDG-SUVR. The main finding of the present study is that STN-DBS increases FDG-SUVR in many subcortical and cortical regions including the target area of surgery, pallidum, caudate nuclei, and associative cortices. In comparison with CONT, FDG-SUVR was depressed in 27% of the brain areas under investigation in DBS_OFF, 90% of which recovered a 'control' activity in DBS_ON including in the STN area. Decreased FDG-SUVR persisted in posterior associative cortices in DBS_ON, but this was not predictive of dementia at follow-up on average 81 months after surgery. Although these conclusions should be restricted to PD patients who benefit the most from STN-DBS and should be confirmed using quantitative FDG-PET data, these novel results contribute to a better understanding of

the mechanisms underlying STN-DBS clinical benefits/limitations and provide new data on PD pathophysiology.

Acknowledgements

The authors thank all patients for agreeing to participate in this study. GG is a Senior Research Associate at the Fonds National de la Recherche Scientifique de Belgique (FRS-FNRS). The authors are grateful to Mrs Aurélie Dessoullières for her help in data management.

Disclosure/conflict of interest

The authors declare no conflict of interest.

References

Alexander GE, Crutcher MD (1990) Functional architecture of basal ganglia circuits: neural substrates of parallel processing. *TINS* 13:266–73

Arai N, Yokochi F, Ohnishi T, Momose T, Okiyama R, Taniguchi M, Takahashi H, Matsuda H, Ugawa Y (2008) Mechanisms of unilateral STN-DBS in patients with Parkinson's disease: a PET study. *J Neurol* 255:1236–43

Asanuma K, Tang C, Ma Y, Dhawan V, Mattis P, Edwards C, Kaplitt MG, Feigin A, Eidelberg D (2006) Network modulation in the treatment of Parkinson's disease. *Brain* 129:2667–78

Ashburner J (2007) A fast diffeomorphic image registration algorithm. *Neuroimage* 38:95–113

Ballanger B, Jahanshahi M, Broussolle E, Thobois S (2009) PET functional imaging of deep brain stimulation in movement disorders and psychiatry. *J Cereb Blood Flow Metab* 29:1743–54

Berding G, Odin P, Brooks DJ, Nikkhah G, Matthies C, Peschel T, Shing M, Kolbe H, van Den HJ, Fricke H, Dengler R, Samii M, Knapp WH (2001) Resting regional cerebral glucose metabolism in advanced Parkinson's disease studied in the off and on conditions with [(18)F]FDG-PET. *Mov Disord* 16:1014–22

Borghammer P, Cumming P, Aanerud J, Forster S, Gjedde A (2009) Subcortical elevation of metabolism in Parkinson's disease–a critical reappraisal in the context of global mean normalization. *Neuroimage* 47:1514–21

Campbell MC, Karimi M, Weaver PM, Wu J, Perantie DC, Golchin NA, Tabbal SD, Perlmutter JS, Hershey T (2008) Neural correlates of STN DBS-induced cognitive variability in Parkinson disease. *Neuropsychologia* 46:3162–9

Ceballos-Baumann A, Boecker H, Bartenstein P, von Falkenhayn I, Riescher H, Conrad B, Moringlane JR, Alesch F (1999) A positron emission tomographic study of subthalamic nucleus stimulation in Parkinson's disease. *Arch Neurol* 56:997–1003

DeLong MR (1990) Primate models of movement disorders of basal ganglia origin. *Trends Neurosci* 13:281–5

Eidelberg D, Moeller JR, Dhawan V, Spetsieris P, Takikawa S, Ishikawa T, Chaly T, Robeson W, Margouleff D, Przedborski S, Fahn S (1994) The metabolic topography of parkinsonism. *J Cereb Blood Flow Metab* 14:783–801

Emre M, Aarsland D, Brown R, Burn DJ, Duyckaerts C, Mizuno Y, Broe GA, Cummings J, Dickson DW, Gauthier S, Goldman J, Goetz C, Korczyn A, Lees A, Levy R, Litvan I, McKeith I, Olanow W, Poewe W, Quinn N, Sampaio C, Tolosa E, Dubois B (2007) Clinical diagnostic criteria for dementia associated with Parkinson's disease. *Mov Disord* 22:1689–707

Fasano A, Romito LM, Daniele A, Piano C, Zinno M, Bentivoglio AR, Albanese A (2010) Motor and cognitive outcome in patients with Parkinson's disease 8 years after subthalamic implants. *Brain* 133:2664–76

Folstein MF, Folstein SE, MsHugh PR (1975) 'Mini-Mental State': a practical method for grading the cognitive state of patients for the clinician. *J Psychiatr Res* 12:189–98

Friston KJ, Frith CD, Liddle PF, Dolan RJ, Lammertsma AA, Frackowiak RS (1990) The relationship between global and local changes in PET scans. *J Cereb Blood Flow Metab* 10:458–66

Garraux G, Salmon E, Degueldre C, Lemaire C, Laureys S, Franck G (1999) Comparison of impaired subcortico-frontal metabolic networks in normal aging, subcortico-frontal dementia, and cortical frontal dementia. *Neuroimage* 10:149–62

Geday J, Ostergaard K, Johnsen E, Gjedde A (2009) STN-stimulation in Parkinson's disease restores striatal inhibition of thalamocortical projection. *Hum Brain Mapp* 30:112–21

Haslinger B, Kalteis K, Boecker H, Alesch F, Ceballos-Baumann AO (2005) Frequency-correlated decreases of motor cortex activity associated with subthalamic nucleus stimulation in Parkinson's disease. *Neuroimage* 28:598–606

Hilker R, Voges J, Weber T, Kracht LW, Roggendorf J, Baudrexel S, Hoevels M, Sturm V, Heiss WD (2008) STN-DBS activates the target area in Parkinson disease: an FDG-PET study. *Neurology* 71:708–13

Hilker R, Voges J, Weisenbach S, Kalbe E, Burghaus L, Ghaemi M, Lehrke R, Koulousakis A, Herholz K, Sturm V, Heiss WD (2004) Subthalamic nucleus stimulation restores glucose metabolism in associative and limbic cortices and in cerebellum: evidence from a FDG-PET study in advanced Parkinson's disease. *J Cereb Blood Flow Metab* 24:7–16

Hughes AJ, Daniel SE, Kilford L, Lees AJ (1992) Accuracy of clinical diagnosis of idiopathic Parkinson's disease: a clinico-pathological study of 100 cases. *J Neurol Neurosurg Psychiatry* 55:181–4

Jenkinson N, Nandi D, Muthusamy K, Ray NJ, Gregory R, Stein JF, Aziz TZ (2009) Anatomy, physiology, and pathophysiology of the pedunculopontine nucleus. *Mov Disord* 24:319–28

Kalbe E, Voges J, Weber T, Haarer M, Baudrexel S, Klein JC, Kessler J, Sturm V, Heiss WD, Hilker R (2009) Frontal FDG-PET activity correlates with cognitive outcome after STN-DBS in Parkinson disease. *Neurology* 72:42–9

Karimi M, Golchin N, Tabbal SD, Hershey T, Videen TO, Wu J, Usche JW, Revilla FJ, Hartlein JM, Wernle AR, Mink JW, Perlmutter JS (2008) Subthalamic nucleus stimulation-induced regional blood flow responses correlate with improvement of motor signs in Parkinson disease. *Brain* 131:2710–9

Krack P, Batir A, Van Blercom N, Chabardes S, Fraix V, Ardouin C, Koudsie A, Limousin PD, Benazzouz A, LeBas JF, Benabid AL, Pollak P (2003) Five-year follow-up of bilateral stimulation of the subthalamic nucleus in advanced Parkinson's disease. *N Engl J Med* 349:1925–34

Limousin P, Greene J, Pollak P, Rothwell J, Benabid A-L, Frackowiak R (1997) Changes in cerebral activity pattern due to subthalamic nucleus or internal pallidum

stimulation in Parkinson's disease. *Ann Neurol* 42: 283–91

Lyoo CH, Jeong Y, Ryu YH, Rinne JO, Lee MS (2010) Cerebral glucose metabolism of Parkinson's disease patients with mild cognitive impairment. *Eur Neurol* 64:65–73

Ma Y, Tang C, Spetsieris PG, Dhawan V, Eidelberg D (2007) Abnormal metabolic network activity in Parkinson's disease: test-retest reproducibility. *J Cereb Blood Flow Metab* 27:597–605

Magistretti PJ, Pellerin P (1999) Cellular mechanisms of brain energy metabolism and their relevance to functional brain imaging. *Phil Trans R Soc Lond B* 354:1155–63

Maquet P, Dive D, Salmon E, von Frenckel R, Franck G (1990) Reproducibility of cerebral glucose utilization measured by PET and the [18F]-2-fluoro-2-deoxy-d-glucose method in resting, healthy human subjects. *Eur J Nucl Med* 16:267–73

Montgomery Jr EB, Gale JT (2008) Mechanisms of action of deep brain stimulation (DBS). *Neurosci Biobehav Rev* 32:388–407

Nofzinger EA, Buysse DJ, Miewald JM, Meltzer CC, Price JC, Sembrat RC, Ombao H, Reynolds CF, Monk TH, Hall M, Kupfer DJ, Moore RY (2002) Human regional cerebral glucose metabolism during non-rapid eye movement sleep in relation to waking. *Brain* 125:1105–15

Payoux P, Remy P, Damier P, Miloudi M, Loubinoux I, Pidoux B, Gaura V, Rascol O, Samson Y, Agid Y (2004) Subthalamic nucleus stimulation reduces abnormal motor cortical overactivity in Parkinson disease. *Arch Neurol* 61:1307–13

Rocher AB, Chapon F, Blaizot X, Baron JC, Chavoix C (2003) Resting-state brain glucose utilization as measured by PET is directly related to regional synaptophysin levels: a study in baboons. *Neuroimage* 20:1894–8

Sestini S, Scotto dL, Ammannati F, De Cristofaro MT, Passeri A, Martini S, Pupi A (2002) Changes in regional cerebral blood flow caused by deep-brain stimulation of the subthalamic nucleus in Parkinson's disease. *J Nucl Med* 43:725–32

Thie JA (2004) Understanding the standardized uptake value, its methods, and implications for usage. *J Nucl Med* 45:1431–4

Trost M, Su S, Su P, Yen RF, Tseng HM, Barnes A, Ma Y, Eidelberg D (2006) Network modulation by the subthalamic nucleus in the treatment of Parkinson's disease. *Neuroimage* 31:301–7

Vafaee MS, Ostergaard K, Sunde N, Gjedde A, Dupont E, Cumming P (2004) Focal changes of oxygen consumption in cerebral cortex of patients with Parkinson's disease during subthalamic stimulation. *Neuroimage* 22:966–74

Wang J, Ma Y, Huang Z, Sun B, Guan Y, Zuo C (2010) Modulation of metabolic brain function by bilateral subthalamic nucleus stimulation in the treatment of Parkinson's disease. *J Neurol* 257:72–8

Yakushev I, Hammers A, Fellgiebel A, Schmidtmann I, Scheurich A, Buchholz HG, Peters J, Bartenstein P, Lieb K, Schreckenberger M (2009) SPM-based count normalization provides excellent discrimination of mild Alzheimer's disease and amnestic mild cognitive impairment from healthy aging. *Neuroimage* 44:43–50

Supplementary Information accompanies the paper on the Journal of Cerebral Blood Flow & Metabolism website (http://www.nature.com/jcbfm)